Sensitivity Analysis of the Non-Linear Liouville Equation

Florian Seitz, Hansjörg Kutterer
Deutsches Geodätisches Forschungsinstitut (DGFI), Marstallplatz 8, D-80539 Munich, Germany
E-Mail: florian.seitz@dgfi.badw.de

Abstract. The non-linear gyroscopic model DyMEG has been developed at DGFI in order to study the interactions between geophysically and gravitationally induced polar motion and the Earth's free wobbles, in particular the Chandler oscillation. The model is based on a triaxial ellipsoid of inertia. It does not need any explicit information concerning amplitude, phase, and period of the Chandler oscillation. The characteristics of the Earth's free polar motion are reproduced by the model from rheological and geometrical parameters. Therefore, the traditional analytical solution is not applicable, and the Liouville equation is solved numerically as an initial value problem. The gyro is driven by consistent atmospheric and oceanic angular momenta. Mass redistributions influence the free rotation by rotational deformations. In order to assess the dependence of the numerical results on the initial values and rheological or geometrical input parameters like the Love numbers and the Earth's principal moments of inertia, a sensitivity analysis has been performed. The study reveals that the pole tide Love number k_2 is the most critical model parameter. The dependence of the solution on the other mentioned parameters is marginal.

Keywords. Earth Rotation, Gyroscopic Model, Liouville Differential Equation, Critical Parameters, Sensitivity Analysis.

1 Introduction

The non-linear gyroscopic model DyMEG (Dynamic Model for Earth Rotation and Gravity) has been developed at DGFI in order to study the dynamics of the Earth system based on the interactions between its individual components. Among these are the atmosphere, the ocean, and the solid Earth. Besides, the influences of sun and moon are considered.

Mass motions outside and inside the Earth are due to geophysical processes and gravitational influences of celestial bodies. They affect the Earth's rotation on sub-daily to secular time scales by polar motion and length-of-day variations (ΔLOD). These variations are superposed by free wobbles of the Earth such as the Chandler oscillation.

DyMEG is based on the balance of angular momentum in the Earth system. The characteristics of Earth rotation are generated by means of rheological and geometrical parameters. No explicit information about amplitude, phase, and period of the Earth's free polar motion is needed as the Liouville differential equation is solved numerically by means of a Runge-Kutta-Fehlberg method (Seitz and Kutterer, 2002; Seitz et al., 2004). In the present investigation, the sensitivity of the solution is discussed with respect to some model parameters which are entered into the model. In particular, the effects of the pole tide Love number k_2, the initial values for the numerical solution and the modification of the initial tensor of inertia of the basic Earth model are discussed.

2 Configuration of DyMEG

2.1 The Liouville Differential equation

With respect to a terrestrial reference system, the Earth's reaction on mass redistributions can be described by the Liouville differential equation:

$$\frac{\mathrm{d}}{\mathrm{dt}}\left(\underline{\mathbf{I}}\,\boldsymbol{\omega}+\mathbf{h}\right)+\boldsymbol{\omega}\times\left(\underline{\mathbf{I}}\,\boldsymbol{\omega}+\mathbf{h}\right)=\mathbf{L}\,. \qquad (1)$$

The vector $\boldsymbol{\omega}(t)$ denotes the rotation vector of the terrestrial system with respect an inertial system. Temporal variations of the Earth's rotation are interpreted as small deviations from a uniform rotation. In the terrestrial system, the coordinates of the Earth rotation vector are expressed by $\boldsymbol{\omega}(t)=\Omega\cdot\left(m_1(t),m_2(t),1+m_3(t)\right)$ where $\Omega\approx 2\pi/$ 86164 s is the approximate angular velocity of the terrestrial system. Small deviations of the instantaneous Earth's rotation axis from the uniform rotation are denoted by the dimensionless quantities m_i(i = 1,

2, 3). The z-axis of the terrestrial reference system is directed approximately towards the Earth's maximum moment of inertia C, the x-axis points towards the Greenwich meridian and the y-axis towards 90°E.

Geophysical and gravitational forces cause motions of masses in individual system components. They show up as changes of the Earth's tensor of inertia $\underline{\mathbf{I}}(t)$ and angular momentum $\mathbf{h}(t)$ with respect to the rotating reference system. The vector $\mathbf{L}(t)$ on the right-hand side of Eq. (1) denotes torques caused by direct gravitational forces of Sun and Moon.

The tensor of inertia $\underline{\mathbf{I}}(t)$ is composed of two components $\underline{\mathbf{I}}_0$ and $\Delta\underline{\mathbf{I}}(t)$, where $\underline{\mathbf{I}}_0$ is the approximate tensor of inertia of the Earth. With respect to the principal axes of inertia, $\underline{\mathbf{I}}_0$ is given by

$$\underline{\mathbf{I}}_0 = \begin{pmatrix} A & 0 & 0 \\ 0 & B & 0 \\ 0 & 0 & C \end{pmatrix}, \qquad (2)$$

where A and B are the equatorial principal moments of inertia ($C>B>A$). $\Delta\underline{\mathbf{I}}(t)$ contains perturbations of $\underline{\mathbf{I}}_0$ due to mass redistributions. The principal axes of inertia and the axes of the terrestrial reference system do not coincide because the axis of the minimum equatorial moment of inertia A points approximately towards 345° longitude (Marchenko and Schwintzer, 2003). This divergence is taken into account by means of a rotation. The dependence of the numerical solution on the values for A, B, and C and on the orientation of the principal axes of inertia is investigated in this paper.

2.2 Free rotation of the gyroscopic model

In order to study the interactions of forced and free wobbles of the Earth, an analytical solution of the Liouville equation is not possible because the Earth's free polar motion is determined within the gyroscopic model by rheological and geometrical parameters (Seitz et al, 2004).

The free wobble of the Earth is lengthened from the Euler period of 304 days (which would be the period if the Earth were a rigid body) to the observed Chandler period of about 434 days due to the influence of rotational deformations (pole tides). This back-coupling mechanism of rotational variations causes perturbations of the second-degree spherical harmonic geopotential coefficients ΔC_{21} and ΔS_{21} (McCarthy, 2003) which are directly linked to $\Delta\underline{\mathbf{I}}(t)$ (Moritz and Mueller, 1987).

$$\Delta C_{21} = -\frac{\Omega^2 a^3}{3GM}\left(\Re(k_2)\cdot m_1 + \Im(k_2)\cdot m_2\right)$$

$$\Delta S_{21} = -\frac{\Omega^2 a^3}{3GM}\left(\Re(k_2)\cdot m_2 - \Im(k_2)\cdot m_1\right)$$

Here, a denotes the Earth's mean equatorial radius, M is the total mass of the Earth and G is the gravitational constant. The effects on the centrifugal potential due to the rheological characteristics of the model body are described by the complex pole tide Love number k_2, which includes the effects of mantle anelasticity and ocean pole tides. Both period and damping of the Chandler oscillation strongly depend on the value of k_2. Its influence on the numerical results is discussed in section 3.1.

In the following, a simple Earth model is employed. It consists of an anelastic mantle and a spherical liquid core which are assumed to be fully decoupled. For investigations of polar motion, this simplification is justified on time scales which are longer than one day (Brzezinski, 2001). Therefore, the principal moments of inertia A, B, and C in Eq. (2) are replaced by A_m, B_m, and C_m which are attributed to the mantle alone (Sasao et al., 1980).

Initial values $m_i(t = t_0)$ for the first time step are deduced from the geodetically observed time series C04 of the IERS. The transformation from the C04-values which describe the celestial ephemeries pole (CEP) with respect to the IERS reference pole and m_i was given by Gross (1992).

2.3 Atmospheric and Oceanic excitation

DyMEG is driven by variations of the atmospheric and oceanic angular momentum. The indirect effect due to load deformations is computed by Green's functions. For atmospheric and oceanic forcing, two independent consistent model combinations are considered.

First, atmospheric data based on the reanalyses of the National Centers of Environmental Prediction (NCEP) (Kalnay et al., 1996) were applied in combination with the ocean model ECCO (Stammer et al., 2003). The combination NCEP + ECCO is a consistent representation of dynamics and mass motions in the subsystems atmosphere and ocean because NCEP forcing fields are used for the computation of ocean dynamics in ECCO. As atmospheric pressure forcing is excluded, the ocean's response to pressure variations is assumed to be inverse barometric. The simulations cover a range of 23 years from 1980 until 2002.

Second, the atmospheric model ECHAM3-T21 GCM (Roeckner et al., 1992), which is driven by observed sea surface temperature (SST) fields, was

used in combination with the ocean model OMCT for circulation and tides (Thomas et al., 2001) which is driven by ECHAM3. Both models and their coupling are described in detail by Seitz et al. (2004). As atmospheric pressure forcing is taken into account by OMCT, the two considered model combinations differ with respect to the pressure coupling. The ECHAM3 + OMCT simulations cover a range of 22 years from 1973 until 1994.

As the NCEP data set is based on atmospheric observations, the combination NCEP + ECCO is expected to correspond better with reality than ECHAM3 + OMCT. The latter models are completely free. Apart from the initial SST-boundary conditions, the dynamics of the atmosphere and the ocean are solely based on model physics. However, it was shown that the polar motion time series resulting from DyMEG are in good agreement with the observations (Seitz et al., 2004).

3 Sensitivity Analysis

3.1 Effect of the pole tide Love number k_2

In order to assess the influence of the pole tide Love number k_2 on polar motion, several model runs, which differ with respect to the value of k_2, were performed. As DyMEG accounts for the effects of equilibrium ocean pole tides and mantle anelasticity, the effective pole tide Love number k_2 is composed of three components:

$$k_2 = k_2^* + \Delta k_2^O + \Delta k_2^A$$

Here, k_2^* denotes a Love number which would be appropriate for a purely elastic Earth. The dynamic response of the ocean as well as the influence of mantle anelasticity are taken into account by adding the supplementary Love numbers Δk_2^O and Δk_2^A, respectively (Smith and Dahlen, 1980). Dynamic effects of the core are neglected because core and mantle are considered decoupled. In DyMEG, the approximate values k_2^* = 0.3, Δk_2^O = 0.044, and Δk_2^A = 0.012 + 0.0035i (Mathews et al., 2002; McCarthy, 2003) are introduced. As the anelastic response of the mantle on rotational variations is accompanied by energy dissipation, the supplement Δk_2^A is complex. As a consequence, the Chandler wobble is a damped oscillation which would diminish if it was not continuously excited.

In the following, the dependence of the numerical solution on the real and imaginary parts of k_2 is studied separately. First, $\Re(k_2)$ was varied from 0.310 to 0.380 in 35 equidistant steps of 0.002 while $\Im(k_2)$ = 0.0035 was kept unchanged. DyMEG was driven by atmospheric and oceanic excitation (NCEP + ECCO) including loading and tidal deformations between 1980 and 2002. In Fig. 1 the resulting time series of the x-component of polar motion are shown for the different values of $\Re(k_2)$. As both annual and Chandler wobbles are almost circular, the y-component looks similar.

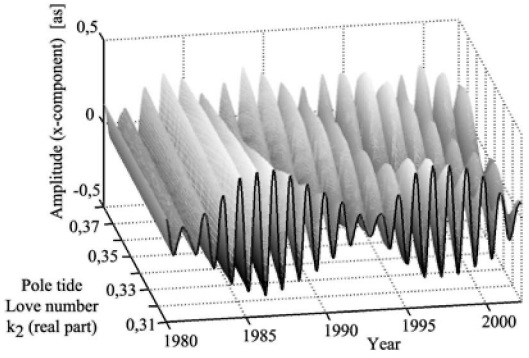

Fig. 1: Resulting time series of polar motion (x-component) for NCEP + ECCO forcing, using different values of $\Re(k_2)$.

As clearly visible, the real part of k_2 has an influence on both the period and the amplitude of the Chandler oscillation and therefore causes a shift of the characteristic beat of free and forced oscillations. From spectral analyses of the time series by means of Fourier transformation, the relation between $\Re(k_2)$ and the Chandler period was obtained (Fig. 2, solid black line). Maximum agreement with the observed Chandler period of 434 days is reached for $\Re(k_2)$ = 0.3520. Here, the correlation between the model time series for polar motion and C04 reaches 0.97. The relation between the Chandler period of the NCEP + ECCO forced model simulations and $\Re(k_2)$ is obviously non-linear.

In order to find the reason for the non-linear relationship, the experiment was repeated without any forcing, i.e. only the effect of rotational deformations was considered. Then DyMEG produces a damped oscillation with periods between 400 and 455 days, respectively. The resulting relation between $\Re(k_2)$ and the Chandler period (Fig. 2, dotted black line) is linear. Accordingly, the non-linearity in the NCEP + ECCO case is due to the interaction of free and forced polar motion. A similar relation between $\Re(k_2)$ and the Chandler period was derived from ECHAM3 + OMCT forced model runs. Neither in NCEP + ECCO nor in ECHAM3 + OMCT, there is increased excitation power in the Chandler frequency band. Nevertheless, there is a significant impact on the Chandler period.

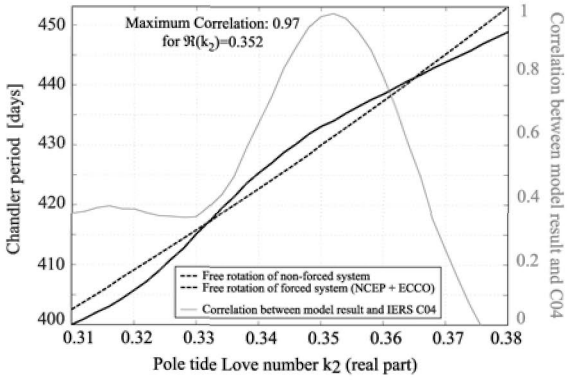

Fig. 2: Relation between $\Re(k_2)$ and the Chandler period as produced by DyMEG in case of forced and unforced conditions. Maximum correlation with the C04 series (scale on the right) is reached for $\Re(k_2) = 0.3520$.

A similar analysis was performed for the imaginary part of k_2. The value of the real part was set to 0.3520. The imaginary part $\Im(k_2)$ was increased equidistantly from 0 (no damping) to 0.0060. A small value of $\Im(k_2)$ causes a slow decrease of the Chandler amplitude, whereas a large value of $\Im(k_2)$ leads to a strong diminution of the Chandler wobble after few years. Unforced results of DyMEG feature damped oscillations, which have a constant period of 434 days but differ with respect to damping. In general, damping is expressed in terms of a so-called quality factor Q. From the damped oscillations of the unforced results, the factor Q was assessed by a least-squares fit (Seitz et al., 2004). For $\Im(k_2) = 0$, Q moves towards infinity, for $\Im(k_2) = 0.0060$ its value is 48 (Fig. 3).

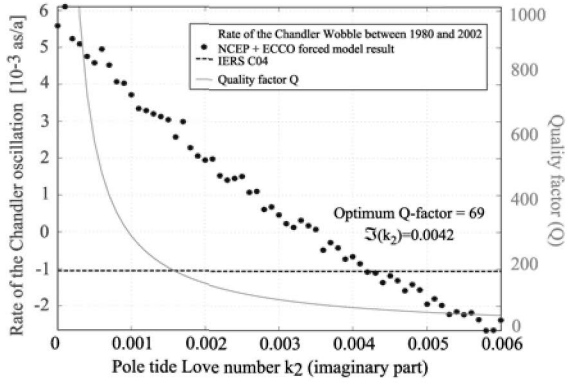

Fig. 3: Relation between $\Im(k_2)$ and the rate of the Chandler amplitude from 1980 until 2002. Optimum agreement between C04 (dotted) and the model result is achieved for $\Im(k_2) = 0.0042$ ($Q = 69$).

In order to assess the optimum damping for the NCEP + ECCO driven system, an annual oscillation with constant amplitude and a Chandler oscillation with a period of 434 days together with an amplitude rate were fit to the model result by means of least-squares adjustment. The resulting Chandler amplitude rates from each model run were compared with the respective value derived from C04 for the time 1980 - 2002 (Fig. 3). Optimum agreement was achieved for $\Im(k_2) = 0.0042$ which corresponds to a quality factor of $Q = 69$. The observed amplitude rate of the Chandler wobble between 1980 and 2002 is -1×10^{-3} as/a.

For ECHAM3 + OMCT, maximum agreement was reached for $\Im(k_2) = 0.0043$ ($Q = 68$) between 1975 and 1994. Hence, the power of the respective excitation series seems slightly higher in this case. But the difference between both model runs is marginal. Summing up the above results, the pole tide Love number k_2 which will be used in the further investigations with DyMEG is set to 0.3520 + 0.0042i.

3.2 Effect of the initial values

In DyMEG, the Liouville differential equation is solved by numerical integration. Hence, initial values $m_i(t = t_0)$ have to be provided. As mentioned above, the initial values are deduced from the C04 series of the IERS. In order to assess the effect of inaccurate initial values on the solution, each of the $m_i(t = t_0)$ was independently varied by uniformly distributed random numbers within $\pm 3\sigma_i$ around the respective C04 value. The standard deviations σ_i of each m_i were calculated from an interval of 30 days around the starting date $t = t_0$. Different starting dates were considered. The simulations were performed in half-yearly steps from 1973 until 1994 for ECHAM3 + OMCT and from 1980 until 2001 for NCEP + ECCO.

This investigation showed that the modification of the initial values within the $\pm 3\sigma_i$-interval for a single starting point does not have a large effect on the resulting time series. In general, the results of 30 model runs which were performed for each of the atmosphere-ocean combinations showed similar results. Deviations between different time series are maximum at the beginning of the simulations (due to the starting situation). But as convergence increases with time, DyMEG seems to reach a steady state.

However, the choice of the starting date seems to be more critical. Fig. 4 displays RMS values of the difference between the model result and C04 for polar motion (x-component) as well as the corresponding correlations against the varying starting date of the simulation. The model runs end at 31.12.1994 (ECHAM3 + OMCT) and 1.3.2002 (NCEP + ECCO).

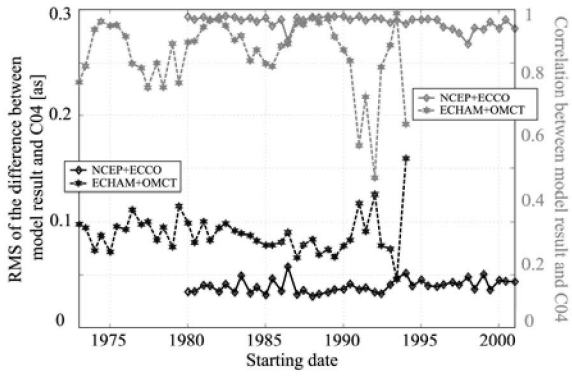

Fig. 4: RMS values of the difference between model results and C04 (black) and respective correlations (grey) for different starting dates.

In general, the NCEP + ECCO results are in better agreement with C04 than those of ECHAM3 + OMCT. Obviously, certain starting dates lead to better results than other ones. For ECCO + NCEP, a start at 1.6.1986 is disadvantageous whereas the neighbouring starting dates lead to good results. For ECHAM3 + OMCT the correlations show an oscillation, which is not visible in the RMS values. This oscillation does not show up in the case of NCEP + ECCO. Accordingly, the amplitudes of polar motion seem to be less affected than the phases and frequencies. During the last few years of the respective simulations, the correlations decrease because the considered parts of the polar motion series are rather short. Hence this effect seems to be an artefact.

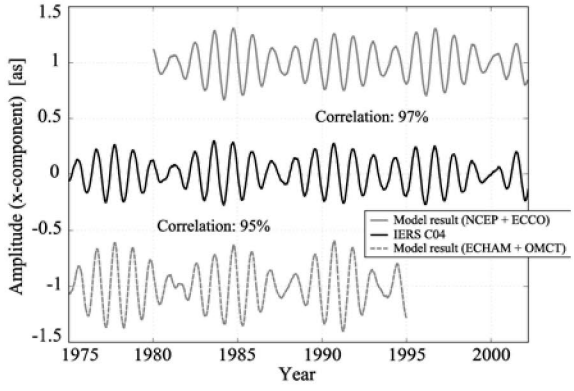

Fig. 5: Model results for DyMEG driven by NCEP + ECCO (top) and ECHAM3 + OMCT (bottom) in comparison with the geodetic observations C04 (middle). For better comparability, the model results are shifted by ±1as.

If the simulations are started at advantageous dates, the model results for polar motion are in good agreement with geodetic observations (Fig. 5). The correlations between the C04 values and the two displayed model runs are 0.95 and 0.97 respectively. As the annual signal of the ECHAM3 + OMCT result is too strong compared to the observations, the RMS of the difference to C04 is higher than for NCEP + ECCO (cf. Fig. 4).

3.3 Effect of variations in the initial tensor of inertia of the basic Earth ellipsoid

The influence of the choice of $\underline{\mathbf{I}}_0$ on the model results for polar motion was tested in two steps.

First, the model results for a triaxial ellipsoid of inertia ($A \neq B$) were contrasted with a simplified biaxial ($A = B$) solution. NCEP + ECCO forcing was applied in both cases. Although the difference between A and B is marginal, it was found that the Chandler period is shortened about two days if a rotationally symmetric ellipsoid of inertia $\underline{\mathbf{I}}_0$ is introduced into DyMEG. Vice versa, in order to lengthen the biaxial Chandler period to the value derived from the triaxial approach, the pole tide Love number has to be adapted (cf. 3.1). According to the results of this study, the appropriate value for $\Re(k_2)$ is 0.3550 in the case of a biaxial ellipsoid of inertia. The results are compiled in Table 1.

Table 1. Periods of the free Earth rotation as derived from DyMEG for a biaxial and triaxial ellipsoid of inertia $\underline{\mathbf{I}}_0$ in dependence of $\Re(k_2)$

	$\Re(k_2) = 0.3520$	$\Re(k_2) = 0.3550$
$A = B$	432	434
$A \neq B$	434	436

In a second step, the values of A, B, and C were changed as well as the directions of the principal axes of inertia with respect to the axes of the terrestrial reference system. Therefore, estimates of the Earth's tensor of inertia were introduced which are based on the recent gravity field solutions JGM-3, EGM96, GRIM5-S1, and GRIM5-S1CH1 (Marchenko and Schwintzer, 2003). In these solutions, the direction $\lambda(A)$ of the principal axis of inertia for the equatorial moment A varies between 345.0709° and 345.0712°. In order to study the sensitivity of DyMEG with respect to $\lambda(A)$, this angle was increased from 344.5° to 345.5° in 50 equidistant steps.

Neither the variation of A, B, and C nor the variation of $\lambda(A)$ within these reasonable limits led to significant changes of the resulting polar motion series. Therefore these parameters of the triaxial tensor of inertia $\underline{\mathbf{I}}_0$ are considered uncritical.

4. Conclusions

The sensitivity of DyMEG with respect to several input parameters as well as the corresponding reliability of the numerical results were assessed within this paper.

The results showed that period and damping of the Chandler wobble as derived from the model strongly depend on the pole tide Love number k_2. From various model runs, the value $k_2 = 0.3520 + 0.0042i$ was found to yield optimum agreement of the model result for polar motion with the C04 series of the IERS. While the value of the real part of k_2 is in good agreement with recent studies, the value of the imaginary part slightly differs from the one given in McCarthy (2003).

The sensitivity of the model Chandler period with respect to the real part of k_2 is very high. A change of this parameter by 1% results in a shift of the period of about two days. Hence, the inference from the Chandler period to $\Re(k_2)$ is relatively precise.

So far, only atmospheric and oceanic angular momentum variations were considered in DyMEG. Mass redistributions in other components of the Earth system like, e.g., land hydrology are still lacking. Hence, oscillations caused by these effects cannot be reproduced by the model. This might yield biases and thus affect the fitting procedure of the deformation Love number.

The variation of the triaxial initial tensor of inertia $\underline{\mathbf{I}}_0$ as well as the modification of the initial values $m_i(t = t_0)$ did not significantly change the results. However, the system is sensitive to the starting date. The correlation between the results from successive NCEP + ECCO driven model runs and C04 showed only slight variations whereas the ECHAM3 + OMCT forced results strongly depend on the starting date. The dependence of the quality of the resulting time series on the starting date will be subject to further investigations. When the simulations are started at advantageous dates the correlation between the model time series and the C04 series reaches 0.95 for ECHAM3 + OMCT and 0.97 for NCEP + ECCO (Fig. 5). As both resulting polar motion series show an undamped beat between free and forced polar motion, it can be concluded, that the atmospheric and oceanic excitation series are able to maintain the Chandler amplitude.

Acknowledgements

This paper was developed within a project funded by DFG grant DR 143/10. The authors thank M. Thomas (Technische Universität Dresden) and J. Stuck (Universität Bonn) for providing OMCT and ECHAM3 data sets. NCEP reanalysis data was provided by the NOAA-CIRES Climate Diagnostics Center, Boulder, Colorado, USA. Moreover we thank B. Richter (DGFI) for proof-reading and his helpful remarks.

References

Brzezinski A. (2001). Diurnal and subdiurnal terms of nutation: a simple theoretical model for a nonrigid Earth. In: Proceedings of the Journées Systèmes de Référence Spatio-temporels 2000, pp. 243-251, ed. Capitaine N., Paris.

Gross R. (1992). Correspondence between theory and observations of polar motion. Geophys. J. Int., 109, 162-170.

Kalnay E., Kanamitsu M., Kistler R. et al. (1996). The NCEP/NCAR 40-Year Reanalysis Project. Bull. Amer. Meteor. Soc., 77, 437-471.

Marchenko A., Schwintzer P. (2003). Estimation of the Earth's tensor of inertia from recent global gravity field solutions. J. Geodesy, 76, 495-509.

Mathews P., Herring T., Buffet B. (2002). Modelling of nutation and precession: New nutation series for nonrigid Earth and insights into the Earth's interior. J. Geophys. Res., 107, 10.1029/2001JB000390.

McCarthy D. (2003). IERS Conventions 2000. IERS Technical Note, Paris.

Moritz H., Mueller I. I. (1987). Earth Rotation. Ungar Publishing Company, New York.

Roeckner E., Arpe K., Bengtsson L. et al. (1992). Simulation of the present-day climate with the ECHAM model: Impact of the model physics and resolution. Tech. Rep. No. 93, Max-Planck-Institut für Meteorologie, Hamburg.

Sasao T., Okubo S., Saito M. (1980). A simple theory on the dynamical effects of a stratified fluid core upon nutational motion of the earth. In: Nutation and the Earth's Rotation, eds. Fedorov E., Smith M., Bender, P., IAU Symposia, 78, D. Reidel, Kiev, 165-183.

Seitz F., Kutterer H. (2002). Numerical Solutions for the Non-Linear Liouville Equation. In: Vistas for Geodesy in the New Millennium, eds. Adam J., Schwarz K.-P., IAG Symposia, 125, Springer, Berlin, 463-468.

Seitz F., Stuck J., Thomas M. (2004). Consistent Atmospheric and Oceanic Excitation of the Earth's Free Polar Motion. To be published in Geophys. J. Int.

Smith M., Dahlen F. (1981). The period and Q of the Chandler wobble. Geophys. J. R. astr. Soc., 64, 223-281.

Stammer D., Wunsch C., Giering R. et al. (2003). Volume, heat and freshwater transports of the global ocean circulation 1993-2000, estimated from a general circulation model constrained by World Ocean Circulation Experiment (WOCE) data. J. Geophys. Res., 108, 10.1029/2001JC001115.

Thomas M., Sündermann J., Maier-Reimer E. (2001). Consideration of ocean tides in an OGCM and its impacts on subseasonal to decadal polar motion excitation. Geophys. Res. Lett., 28, No. 12, 2557-2560.